

Λ_c^+ , Σ_c , Ξ_c and Λ_b hypernuclei in the quark-meson coupling model

K Tsushima^{1,2} * and F C Khanna^{3,4} †

¹Instituto de Física Teórica - UNESP, Rua Pamplona 145, 01405-900, Sao Paulo - SP, Brazil

²Mackenzie University - FCBEE, Rua da Consolacao 930, 01302-907, Sao Paulo - SP, Brazil

³Department of Physics, University of Alberta, Edmonton, Canada, T6G 2J1

⁴TRIUMF, 4004 Wesbrook Mall, Vancouver, British Columbia, Canada, V6T 2A3

Abstract

Charmed (and bottom) hypernuclei are studied in the quark-meson coupling (QMC) model. This completes systematic studies of charmed (Λ_c^+ , Σ_c , Ξ_c), and Λ_b hypernuclei in the QMC model. Effects of the Pauli blocking due to the underlying quark structure of baryons, and the $\Sigma_c N - \Lambda_c N$ channel coupling are phenomenologically taken into account at the hadronic level in the same way as those included for strange hypernuclei. Our results suggest that the Σ_c^{++} and Ξ_c^+ hypernuclei are very unlikely to be formed, while the Λ_c^+ , Ξ_c^0 and Λ_b hypernuclei are quite likely to be formed. For the Σ_c^+ hypernuclei, the formation probability is non-zero though small. A detailed analysis is also made about the phenomenologically introduced Pauli blocking and channel coupling effects for the Σ_c^0 hypernuclei.

*tsushima@ift.unesp.br

†khanna@Phys.UAlberta.CA

1 Introduction

Based on the quark-meson coupling (QMC) model [1], we have recently initiated a systematic study of charmed and bottom hadrons in nuclear matter [2]. The results imply that the formations of B^- -meson nuclear (atomic) bound states, and Λ_c^+ and Λ_b hypernuclei are quite likely. The formations of Λ_c^+ and/or Λ_b hypernuclei were first predicted in mid-1970s by Tyapkin [3], and Dover and Kahana [4]. Later on theoretical studies [5, 6] as well as possibility of experimental observation [7] were made. Further, we have studied [8] the Λ_c^+ and Λ_b hypernuclei by solving equations of motion for a system of hypernuclei, embedding a Λ_c^+ or a Λ_b into the closed shell nuclear core, within the Hartree, mean-field, approximation using the QMC model. The results again support the possible formation of Λ_c^+ and Λ_b hypernuclei.

In this article we present the results for the Σ_c and Ξ_c hypernuclei, as well as some of the Λ_c^+ and Λ_b hypernuclei studied recently [8]. This is an extension of the studies made for the strange hypernuclei [9], and a completion of our systematic study of charmed and bottom hypernuclei [2, 8] in the QMC model. The extension is straightforward, since the heavy baryons (as well as nucleon) are classified by the naive constituent quark model, and QMC can treat them on the same quark-based footing.

One of the other important issues in this study is a role of the u and d light quarks in nuclear medium, in the charmed or bottom baryons containing u and/or d quarks. This concerns the partial restoration of chiral symmetry in nuclear medium for heavy baryons.

Concerning the experimental possibilities, the approved construction of the Japan Hadron Facility (JHF) with a beam energy of 50 GeV, will produce charmed hadrons profusely and bottom hadrons in lesser numbers, but still with an intensity which is comparable to the present hyperon production rates. Although the study of possible existence of charmed and bottom hypernuclei may be in its infancy at present, it is clear that conditions for the experiments to search for such heavy baryon hypernuclei are now becoming realistic, and would be realized at JHF [10]. Thus, it is still meaningful to consider such heavy baryon hypernuclei at this stage for the future experimental studies.

The QMC model (QMC-I), which is used in this study, has been successfully applied to many problems of nuclear physics, such as finite nuclei [11, 12], strange hypernuclei [9], nuclear matter [13], and other problems including hadronic properties in nuclear medium [14, 15, 16, 17, 18, 19, 20]. (See also Refs. [21, 22] for earlier, different versions of QMC, and Ref. [23] for related work.) For example, the model was applied to the study of meson nuclear bound states [15, 16], J/Ψ dissociation in nuclear matter [18], D and \bar{D} production in antiproton-nucleus collisions [19], and kaon properties in nuclear matter and kaon production in heavy ion collisions [20]. Furthermore, although only some limited studies for heavy mesons (not for heavy baryons) with charm in nuclear matter were made by the QCD sum rules (for J/Ψ [24, 25] and $D(\bar{D})$ [26]), a study for heavy baryons containing charm or bottom quarks was made only recently [2] using the QMC model. Furthermore, recent measurements of polarization transfer in the $^4\text{He}(\vec{e}, e'\vec{p})^3\text{H}$ and $^{16}\text{O}(\vec{e}, e'\vec{p})^{15}\text{N}$ reactions performed at MAMI and Jefferson Lab [27], support the medium modification of the proton electromagnetic form factors predicted by the QMC model [17].

There is also another version of the QMC model (QMC-II), where masses of the meson fields are also subject to the medium modification in a self-consistent manner [28]. However, for a proper parameter set (set B) the typical results obtained in QMC-II are very similar to those of QMC-I. The difference is $\sim 16\%$ for the largest case, but typically $\sim 10\%$ or less. (For

the effective masses of the hyperons, the differences between the two versions of QMC turn out to be less than $\sim 8\%$. See also Fig. 2 in Ref. [15] for the differences in the scalar potentials for the η and ω mesons in ^{208}Pb nucleus.) Since we use QMC-I, the differences in these numbers may be regarded as uncertainties in the model.

Certainly, the model has shortcomings that have to be improved eventually. Difficulties to handle the model will increase rapidly in handling the Hartree-Fock approximation even for nuclear matter [29], and further to include the Pauli blocking effect at the quark level. In addition, the $\Sigma N - \Lambda N$ channel coupling effect has not been implemented yet in a consistent manner with the underlying quark degrees of freedom [9]. It should be mentioned that in the case of larger mass number Σ hypernuclei, no narrow states have been observed experimentally, although $^4_{\Sigma}\text{He}$ was confirmed [30]. It is unlikely to find such (narrow) bound states in the present situation, where the experimental analysis [30] supports the suggestion made by Harada [31], that a large isospin dependent Σ -nucleus potential term exists and the $1/A$ (A :baryon number) dependence of that term reduces the likelihood of observing bound states for $A > 5$. This unlikelihood may also arise from the width of Σ state due to strong $\Sigma - \Lambda$ conversion. Furthermore, an application to double hypernuclei has not been attempted, although recently the existence was confirmed for small baryon number nuclei [32]. As an attempt to improve the model, the effect of short-range quark-quark correlations associated with the nucleon overlap was studied in Ref. [33]. With the addition of the correlations, the saturation curve for symmetric nuclear matter was greatly improved at high density. Despite the shortcomings of the model described above, there are some positive aspects of this model, its simplicity and successful applicability, that we feel confident that the QMC model will provide us with a valuable glimpse into the properties of charmed and bottom hypernuclei.

In the QMC model, the interactions between nucleons are mediated by the exchange of scalar (σ) and vector (ω and ρ) fields self-consistently coupled directly to the quarks within those nucleons, but not to the nucleons as in Quantum Hadrodynamics (QHD) [34]. Thus, it can be systematically applied to study the properties of any hadrons in nuclear medium [2, 14] (if they contain u and/or d light quarks). We make use of this advantage of the QMC model, and study the charmed and bottom hypernuclei. We hope that the present study inspires some interest to measure the properties of heavy baryons in nuclear medium, at facilities like JHF, particularly at RHIC (high energy relativistic heavy ion facilities), and in very high energy experiments at CERN and Fermilab.

The organization of this article is as follows. In Section 2, the relativistic formulation of the charmed and bottom hypernuclear system in the QMC model will be explained briefly. A mean-field Lagrangian density and equations of motion will be given in Section 2.1, while charmed and bottom hadrons in nuclear matter will be discussed in Section 2.2. In Section 3, the effects necessary for a realistic calculation for the charmed (bottom) hypernuclei will be described. Spin-orbit potential, and the effect of the Pauli blocking at the quark level will be explained in Sections 3.1 and 3.2, respectively. In addition, $\Sigma_{c,b}N - \Lambda_{c,b}N$ channel coupling effect will be explained in Section 3.2. The results for the charmed and bottom hypernuclei will be presented in Section 4, and finally Section 5 will be devoted to summary and discussion.

2 Charmed and bottom hypernuclei in the QMC model

In this Section, we briefly explain the mean-field equations of motion for a charmed or bottom hypernuclear system, and review some properties of the charmed and bottom baryons in nuclear matter.

2.1 Mean-field equations of motion

We consider static, approximately spherically symmetric charmed and bottom hypernuclei, i.e., closed shell nuclear core plus one charmed or one bottom baryon (heavy baryon) configuration, ignoring non-spherical effects due to the embedded heavy baryon. The existence of the heavy baryon inside or outside of the nuclear core (in particular, Λ_b which interacts relatively strong with core nucleons) breaks spherical symmetry, and one should include this effect in a truly rigorous treatment. We have neglected this effect, since it is not expected to be so important for spectroscopic calculations [35, 36] for the middle and/or large baryon number charmed hypernuclei (but may not be true for Λ_b hypernuclei), and beyond the scope of present study. However, we include the response of the nuclear core arising from the self-consistent calculation, which is a purely relativistic effect [36, 37]. Thus, we always specify the state of the heavy baryon in which the calculation is performed, because the core nucleus response is different due to the self-consistent calculation. (This self-consistent procedure will be applied also when the effective Pauli blocking and/or $\Sigma_{c,b} - \Lambda_{c,b}$ are introduced later.)

We adopt the Hartree, mean-field, approximation. In this approximation the ρNN tensor coupling contributes to a spin-orbit force for a nucleon bound in a static spherical nucleus, although in Hartree-Fock it also contributes a central force [11, 12]. (Furthermore, it gives no contribution for nuclear matter since the meson fields are independent of position and time.) Thus, we ignore the ρNN tensor coupling in this study as in Ref. [9].

A relativistic Lagrangian density for a charmed or a bottom hypernucleus in the QMC model may be given by [9]:

$$\begin{aligned}
\mathcal{L}_{QMC}^{CHY} &= \mathcal{L}_{QMC} + \mathcal{L}_{QMC}^C, \\
\mathcal{L}_{QMC} &= \bar{\psi}_N(\vec{r}) \left[i\gamma \cdot \partial - M_N^*(\sigma) - (g_\omega \omega(\vec{r}) + g_\rho \frac{\tau_3^N}{2} b(\vec{r}) + \frac{e}{2}(1 + \tau_3^N) A(\vec{r})) \gamma_0 \right] \psi_N(\vec{r}) \\
&\quad - \frac{1}{2} [(\nabla \sigma(\vec{r}))^2 + m_\sigma^2 \sigma(\vec{r})^2] + \frac{1}{2} [(\nabla \omega(\vec{r}))^2 + m_\omega^2 \omega(\vec{r})^2] \\
&\quad + \frac{1}{2} [(\nabla b(\vec{r}))^2 + m_\rho^2 b(\vec{r})^2] + \frac{1}{2} (\nabla A(\vec{r}))^2, \\
\mathcal{L}_{QMC}^C &= \sum_{C=\Lambda_c^+, \Sigma_c^{0,+,++}, \Xi_c^{0,+}, \Lambda_b} \bar{\psi}_C(\vec{r}) \left[i\gamma \cdot \partial - M_C^*(\sigma) - (g_\omega^C \omega(\vec{r}) + g_\rho^C I_3^C b(\vec{r}) + e Q_C A(\vec{r})) \gamma_0 \right] \psi_C(\vec{r}), \quad (1)
\end{aligned}$$

where $\psi_N(\vec{r})$ ($\psi_C(\vec{r})$) and $b(\vec{r})$ are respectively the nucleon (charmed or bottom baryon) and the ρ meson (the time component in the third direction of isospin) fields, while m_σ , m_ω and m_ρ are the masses of the σ , ω and ρ meson fields. g_ω and g_ρ are the ω - N and ρ - N coupling constants which are respectively related to (u, d) -quark- ω , g_ω^q , and (u, d) -quark- ρ , g_ρ^q , coupling constants as $g_\omega = 3g_\omega^q$ and $g_\rho = g_\rho^q$ [11, 12]. Note that these meson fields, σ, ω and ρ , represent the quantum numbers and Lorentz structure which mediate the interactions among the nucleons in nuclear medium as in original QHD [34], corresponding, $\sigma \leftrightarrow \phi_0$, $\omega \leftrightarrow V_0$ and $b \leftrightarrow b_0$, and

they may not be directly connected with the physical particles, nor quark model states. Their masses in nuclear medium do not vary in the present treatment of QMC-I. Hereafter we will use notations for the quark flavors, $q \equiv u, d$ and $Q \equiv s, c, b$.

In an approximation where the σ , ω and ρ fields couple only to the u and d quarks, the coupling constants for the heavy baryon are obtained as $g_\omega^C = (n_q/3)g_\omega$, and $g_\rho^C \equiv g_\rho = g_\rho^q$, with n_q being the total number of valence u and d light quarks in the heavy baryon C . I_3^C and Q_C are the third component of the heavy baryon isospin operator and its electric charge in units of the proton charge, e , respectively. The field dependent σ - N and σ - C coupling strengths predicted by the QMC model, $g_\sigma(\sigma) \equiv g_\sigma^N(\sigma)$ and $g_\sigma^C(\sigma)$, related to the Lagrangian density of Eq. (1) are defined by

$$M_N^*(\sigma) \equiv M_N - g_\sigma(\sigma)\sigma(\vec{r}), \quad (2)$$

$$M_C^*(\sigma) \equiv M_C - g_\sigma^C(\sigma)\sigma(\vec{r}), \quad (3)$$

where M_N (M_C) is the free nucleon (heavy baryon) mass. Note that the dependence of these coupling strengths on the applied scalar field must be calculated self-consistently within the quark model [9, 11, 12]. Hence, unlike QHD [34], even though $g_\sigma^C(\sigma)/g_\sigma(\sigma)$ may be 2/3 or 1/3 depending on the number of light quarks in the heavy baryon in free space, $\sigma = 0$, (but only when their bag radii in free space are exactly the same), this will not necessarily be the case in nuclear matter. Explicit expressions for $g_\sigma^C(\sigma)$ and $g_\sigma(\sigma)$ will be given later in Eq. (14). From the Lagrangian density Eq. (1), a set of equations of motion for the heavy baryon hypernuclear system is obtained:

$$[i\gamma \cdot \partial - M_N^*(\sigma) - (g_\omega\omega(\vec{r}) + g_\rho\frac{\tau_3^N}{2}b(\vec{r}) + \frac{e}{2}(1 + \tau_3^N)A(\vec{r}))\gamma_0]\psi_N(\vec{r}) = 0, \quad (4)$$

$$[i\gamma \cdot \partial - M_C^*(\sigma) - (g_\omega^C\omega(\vec{r}) + g_\rho I_3^C b(\vec{r}) + eQ_C A(\vec{r}))\gamma_0]\psi_C(\vec{r}) = 0, \quad (5)$$

$$\begin{aligned} (-\nabla_r^2 + m_\sigma^2)\sigma(\vec{r}) &= -\left[\frac{\partial M_N^*(\sigma)}{\partial\sigma}\right]\rho_s(\vec{r}) - \left[\frac{\partial M_C^*(\sigma)}{\partial\sigma}\right]\rho_s^C(\vec{r}), \\ &\equiv g_\sigma C_N(\sigma)\rho_s(\vec{r}) + g_\sigma^C C_C(\sigma)\rho_s^C(\vec{r}), \end{aligned} \quad (6)$$

$$(-\nabla_r^2 + m_\omega^2)\omega(\vec{r}) = g_\omega\rho_B(\vec{r}) + g_\omega^C\rho_B^C(\vec{r}), \quad (7)$$

$$(-\nabla_r^2 + m_\rho^2)b(\vec{r}) = \frac{g_\rho}{2}\rho_3(\vec{r}) + g_\rho^C I_3^C \rho_B^C(\vec{r}), \quad (8)$$

$$(-\nabla_r^2)A(\vec{r}) = e\rho_p(\vec{r}) + eQ_C\rho_B^C(\vec{r}), \quad (9)$$

where, $\rho_s(\vec{r})$ ($\rho_s^C(\vec{r})$), $\rho_B(\vec{r})$ ($\rho_B^C(\vec{r})$), $\rho_3(\vec{r})$ and $\rho_p(\vec{r})$ are the scalar, baryon, third component of isovector, and proton densities at the position \vec{r} in the heavy baryon hypernucleus [9, 11, 12]. On the right hand side of Eq. (6), $-\left[\partial M_N^*(\sigma)/\partial\sigma\right] \equiv g_\sigma C_N(\sigma)$ and $-\left[\partial M_C^*(\sigma)/\partial\sigma\right] \equiv g_\sigma^C C_C(\sigma)$, where $g_\sigma \equiv g_\sigma(\sigma = 0)$ and $g_\sigma^C \equiv g_\sigma^C(\sigma = 0)$, are a new, and characteristic feature of QMC beyond QHD [34, 41, 42, 43]. The effective mass for the heavy baryon C is defined by

$$\frac{\partial M_C^*(\sigma)}{\partial\sigma} = -n_q g_\sigma^q \int_{bag} d^3x \bar{\psi}_q(\vec{x})\psi_q(\vec{x}) \equiv -n_q g_\sigma^q S_C(\sigma) = -\frac{\partial}{\partial\sigma} [g_\sigma^C(\sigma)\sigma], \quad (10)$$

with the MIT bag model quantities, and the mass stability condition to be satisfied in obtaining the in-medium bag radius [1, 9, 11, 12]:

$$M_C^*(\sigma) = \sum_{j=q,Q} \frac{n_j \Omega_j^* - z_C}{R_C^*} + \frac{4}{3}\pi(R_C^*)^3 B, \quad (11)$$

$$S_C(\sigma) = \frac{\Omega_q^*/2 + m_q^* R_C^* (\Omega_q^* - 1)}{\Omega_q^* (\Omega_q^* - 1) + m_q^* R_C^* / 2}, \quad (12)$$

$$\Omega_q^* = \sqrt{x_q^2 + (R_C^* m_q^*)^2}, \quad \Omega_Q^* = \sqrt{x_Q^2 + (R_C^* m_Q^*)^2}, \quad m_q^* = m_q - g_\sigma^q \sigma(\vec{r}), \quad (13)$$

$$C_C(\sigma) = S_C(\sigma)/S_C(0), \quad g_\sigma^C \equiv n_q g_\sigma^q S_C(0) \equiv \frac{n_q}{3} g_\sigma \Gamma_{C/N} = \frac{n_q}{3} g_\sigma S_C(0)/S_N(0), \quad (14)$$

$$\left. \frac{dM_C^*}{dR_C} \right|_{R_C=R_C^*} = 0. \quad (15)$$

Quantities for the nucleon are similarly obtained by replacing the indices, $C \rightarrow N$, in Eqs. (10) - (15). Approximating the constant, mean meson fields within the bag neglecting the Coulomb force, the wave functions, $\psi_f(x)$ ($f = u, d, s, c, b$), satisfy the Dirac equations for the quarks in the baryon bag centered at a position \vec{r} of the nucleus, ($|\vec{x} - \vec{r}| \leq$ bag radius [15, 16, 20]):

$$\left[i\gamma \cdot \partial_x - (m_q - V_\sigma^q(\vec{r})) - \gamma^0 \left(V_\omega^q(\vec{r}) \pm \frac{1}{2} V_\rho^q(\vec{r}) \right) \right] \begin{pmatrix} \psi_u(x) \\ \psi_d(x) \end{pmatrix} = 0, \quad (16)$$

$$[i\gamma \cdot \partial_x - m_Q] \psi_Q(x) = 0, \quad (17)$$

where, $q = u$ or d , and $Q = s, c$ or b . The constant, mean-field potentials within the bag are defined by $V_\sigma^q(\vec{r}) \equiv g_\sigma^q \sigma(\vec{r})$, $V_\omega^q(\vec{r}) \equiv g_\omega^q \omega(\vec{r})$ and $V_\rho^q(\vec{r}) \equiv g_\rho^q b(\vec{r})$, with g_σ^q , g_ω^q and g_ρ^q the corresponding quark-meson coupling constants. The eigenenergies, $\epsilon_{u,d,Q}$ in units of $1/R_C^*$ are given by

$$\begin{pmatrix} \epsilon_u \\ \epsilon_d \end{pmatrix} = \Omega_q^* + R_C^* \left(V_\omega^q(\vec{r}) \pm \frac{1}{2} V_\rho^q(\vec{r}) \right), \quad \epsilon_Q = \Omega_Q^*, \quad (18)$$

where, Ω_q^* and Ω_Q^* are given in Eq. (13).

In the expressions of the MIT bag quantities Eqs. (11) and (13), z_C , B , $x_{q,Q}$, and $m_{q,Q}$ are the parameters for the sum of the c.m. and gluon fluctuation effects, bag pressure, lowest eigenvalues for the quarks q or Q , respectively, and the corresponding current quark masses. z_N and B (z_C) are fixed by fitting the nucleon (heavy baryon) mass in free space. For the current quark masses we use $(m_{u,d}, m_s, m_c, m_b) = (5, 250, 1300, 4200)$ MeV, where the values for m_c and m_b are the averaged values from Refs. [38] and [39], respectively, and these values were used in Refs. [2, 8, 16, 18, 19]. Then, we obtain the bag pressure $B = (170 \text{ MeV})^4$, by choosing the bag radius for the nucleon in free space $R_N = 0.8$ fm. The quark-meson coupling constants, which are determined so as to reproduce the saturation properties of symmetric nuclear matter are, $(g_\sigma^q, g_\omega^q, g_\rho^q) = (5.69, 2.72, 9.33)$, where $g_\sigma \equiv g_\sigma^N \equiv 3g_\sigma^q S_N(0) = 3 \times 5.69 \times 0.483 = 8.23$ [12]. (See Eq. (14) with the replacement, $C \rightarrow N$.) The parameters z_j , and the bag radii R_j in free space ($j = N, \Lambda, \Sigma, \Xi, \Lambda_c^+, \Sigma_c, \Xi_c, \Lambda_b$) and also some quantities calculated at normal nuclear mater density $\rho_B = 0.15 \text{ fm}^{-3}$, are listed in Table 1, together with the free space masses [40]. (Nuclear mater limit will be discussed in Section 2.2.)

At the hadronic level, the entire information on the quark dynamics is condensed into the effective couplings $C_{N,C}(\sigma)$ of Eq. (6). Furthermore, when $C_{N,C}(\sigma) = 1$, which corresponds to a structureless nucleon or a heavy baryon, the equations of motion given by Eqs. (4) - (9) can be identified with those derived from QHD [41, 42, 43], except for the terms arising from the tensor coupling and the non-linear scalar and/or vector field interactions introduced beyond the naive QHD.

The explicit expressions for coupled differential equations to obtain various fields and baryon wave functions to describe a heavy baryon hypernuclear system, for the spherically

Table 1: The bag parameters, the baryon masses and the bag radii in free space [at normal nuclear matter density, $\rho_B = 0.15 \text{ fm}^{-3}$] z_j, R_j and M_j [R_j^* and M_j^*] ($j = N, \Lambda, \Lambda_c^+, \Sigma_c, \Xi_c, \Lambda_b$), respectively.

j	z_j	M_j (MeV)	R_j (fm)	M_j^* (MeV)	R_j^* (fm)
N	3.295	939.0	0.800	754.5	0.786
Λ	3.131	1115.7	0.806	992.7	0.803
Σ	2.810	1193.1	0.827	1070.4	0.824
Ξ	2.860	1318.1	0.820	1256.7	0.818
Λ_c^+	1.766	2284.9	0.846	2162.5	0.843
Σ_c	1.033	2452.0	0.885	2330.2	0.882
Ξ_c	1.564	2469.1	0.853	2408.0	0.851
Λ_b	-0.643	5624.0	0.930	5502.9	0.928

symmetric nucleus plus one heavy baryon configuration can be obtained by replacing the corresponding indices from hyperon to heavy baryon ($Y \rightarrow C$) in Ref. [9].

2.2 Nuclear matter limit

Here, we summarize the results and discussions given in Refs. [2, 9] for a limit of nuclear matter. New things in this subsection are some results given in Tables 1 and 2, and to inform the similar treatments (parameterizations) also work for charmed and bottom baryons as will be shown in Eqs. (21) and (22), which may not be so trivial. In the nuclear matter limit all meson fields become constant, and we denote the mean-values of the ω and σ fields by $\bar{\omega}$ and $\bar{\sigma}$, respectively. Then, equations for the $\bar{\omega}$ and self-consistency condition for the $\bar{\sigma}$ are given by [1, 11, 12, 13]

$$\bar{\omega} = \frac{4}{(2\pi)^3} \int d^3k \theta(k_F - k) = \frac{g_\omega}{m_\omega^2} \frac{2k_F^3}{3\pi^2} = \frac{g_\omega}{m_\omega^2} \rho_B, \quad (19)$$

$$\bar{\sigma} = \frac{g_\sigma}{m_\sigma^2} C_N(\bar{\sigma}) \frac{4}{(2\pi)^3} \int d^3k \theta(k_F - k) \frac{M_N^*(\bar{\sigma})}{\sqrt{M_N^{*2}(\bar{\sigma}) + k^2}} = \frac{g_\sigma}{m_\sigma^2} C_N(\bar{\sigma}) \rho_s, \quad (20)$$

where $g_\sigma = 3g_\sigma^q S_N(0)$ (see Eq. (14) by the replacement, $C \rightarrow N$), k_F is the Fermi momentum, ρ_B and ρ_s are the baryon and scalar densities, respectively. Note that $M_N^*(\bar{\sigma})$ in Eq. (20), must be calculated self-consistently by the MIT bag model, through Eqs. (10) - (16). This self-consistency equation for the $\bar{\sigma}$ is the same as that in QHD, except that in the latter one has $C_N(\bar{\sigma}) = 1$ [34]. Using the mean field value $\bar{\sigma}$, the corresponding quantity for the heavy baryon C , $C_C(\bar{\sigma})$, can be also calculated using Eqs. (10) - (17) neglecting the effect of a single heavy baryon on the mean field value $\bar{\sigma}$, in infinite nuclear matter.

It has been found that the function $C_j(\bar{\sigma})$ ($j = N, \Lambda, \Sigma, \Xi, \Lambda_c^+, \Sigma_c, \Xi_c, \Lambda_b$) can be parametrized as a linear form in the σ field, $g_\sigma \bar{\sigma}$, for practical calculations [9, 11, 12]:

$$C_j(\bar{\sigma}) = 1 - a_j \times (g_\sigma \bar{\sigma}), \quad (j = N, \Lambda, \Sigma, \Xi, \Lambda_c^+, \Sigma_c, \Xi_c, \Lambda_b). \quad (21)$$

The values obtained for a_j are listed in Table 2. This parameterization works very well up to about three times of normal nuclear matter density $\rho_B \simeq 3\rho_0$ ($\rho_0 \simeq 0.15 \text{ fm}^{-3}$). Then, the

effective masses for the baryon, j , in nuclear matter are well approximated by [9, 11, 12]

$$M_j^* \simeq M_j - \frac{n_q}{3} g_\sigma \left[1 - \frac{a_j}{2} (g_\sigma \bar{\sigma}) \right] \bar{\sigma}, \quad (j = N, \Lambda, \Sigma, \Xi, \Lambda_c^+, \Sigma_c, \Xi_c, \Lambda_b), \quad (22)$$

with n_q being the number of light quarks in the baryon j . For the field strength $g_\sigma \bar{\sigma}$ versus baryon density, one can find in Ref. [11].

Table 2: The slope parameters, a_j ($j = N, \Lambda, \Sigma, \Xi, \Lambda_c^+, \Sigma_c, \Xi_c, \Lambda_b$).

a_j	$\times 10^{-4} \text{ MeV}^{-1}$	a_j	$\times 10^{-4} \text{ MeV}^{-1}$
a_N	8.8	a_{Λ_b}	10.9
a_Λ	9.3	$a_{\Lambda_c^+}$	9.8
a_Σ	9.5	a_{Σ_c}	10.3
a_Ξ	9.4	a_{Ξ_c}	9.9

Next, we discuss briefly the scalar and vector potentials of charmed and bottom baryons in nuclear matter [2]. The scalar (V_s^j) and vector (V_v^j) potentials for the baryon j , in nuclear matter are given by

$$V_s^j = m_j^* - m_j, \quad (23)$$

$$V_v^j = n_q V_\omega^q + I_3^j V_\rho^q, \quad (24)$$

where I_3^j is the third component of isospin projection of the baryon j . Thus, the vector potential for a heavy baryon with charm or bottom quark(s), is equal to that of the hyperon with the same light quark number in the QMC model. Calculated results for the scalar potentials for the baryons in symmetric nuclear matter are shown in Fig. 1, which is taken from Ref. [2] by omitting those for mesons. From the results it is confirmed that the scalar potential for the baryon j , V_s^j , follows a simple light quark number counting rule:

$$V_s^j \simeq \frac{n_q}{3} V_s^N, \quad (25)$$

where n_q is the number of light quarks in the baryon j , and V_s^N is the scalar potential for the nucleon. (See Eq.(23).) It is interesting to note that, the baryons with charm and bottom quarks (Ξ_c is a quark flavor configuration, qsc), show features very similar to those of the corresponding strange hyperons with the same light quark numbers. Then, ignoring the Coulomb force although it is important in a realistic hypernucleus, we may expect that these heavy baryons with charm or bottom quarks, will also form some heavy baryon hypernuclei at this stage, as the strange hyperons do. (Recall that the repulsive, vector potentials are the same for the corresponding hyperons with the same light quark numbers.)

3 Calculations

In this section, we discuss parameters used in the calculations: spin-orbit force in the QMC model, the Pauli blocking effect at the quark level, and the effect of channel coupling, $\Sigma_{c,b}N -$

$\Lambda_{c,b}N$. The parameters are the same as those used in the study of strange hypernuclei [9], except for those related to charmed and bottom hypernuclei given in Section 2, but the treatment is the same as that of Ref. [9]. More detailed discussions may be found in Ref. [9].

3.1 Spin-orbit force in the QMC model

The origin of the spin orbit force for a composite nucleon moving through scalar and vector fields which vary with position is explained in detail in Ref. [11]. For the Λ, Σ and Ξ cases are explained in Ref. [9]. Although the spin-orbit splittings for the nucleon calculated in QMC are already somewhat smaller [11, 12], it was demonstrated that much smaller spin-orbit splittings were obtained for the Λ in QMC [9]. These will turn out to be even smaller for the heavy baryon hypernuclei.

In order to include the spin-orbit potential approximately, e.g., for the Λ_c^+ , we add perturbatively the correction due to the vector potential, $-\frac{2}{2M_{\Lambda_c^+}^{*2}(\vec{r})r} \left(\frac{d}{dr} g_{\omega}^{\Lambda_c^+} \omega(\vec{r}) \right) \vec{l} \cdot \vec{s}$, to the single-particle energies obtained with the Dirac equation, in the same way as that added for the strange hypernuclei [9]. This may correspond to a correct spin-orbit force which is calculated by the underlying quark model [9, 11]:

$$V_{S.O.}^{\Lambda_c^+}(\vec{r})\vec{l} \cdot \vec{s} = -\frac{1}{2M_{\Lambda_c^+}^{*2}(\vec{r})r} \left(\frac{d}{dr} [M_{\Lambda_c^+}^*(\vec{r}) + g_{\omega}^{\Lambda_c^+} \omega(\vec{r})] \right) \vec{l} \cdot \vec{s}, \quad (26)$$

since the Dirac equation at the hadronic level solved in usual QHD-type models leads to:

$$V_{S.O.}^{\Lambda_c^+}(\vec{r})\vec{l} \cdot \vec{s} = -\frac{1}{2M_{\Lambda_c^+}^{*2}(\vec{r})r} \left(\frac{d}{dr} [M_{\Lambda_c^+}^*(\vec{r}) - g_{\omega}^{\Lambda_c^+} \omega(\vec{r})] \right) \vec{l} \cdot \vec{s}, \quad (27)$$

which has the opposite sign for the vector potential, $g_{\omega}^{\Lambda_c^+} \omega(\vec{r})$. The correction to the spin-orbit force in the QMC model, appears due to the structure of the baryon (finite size). This may also be modeled at the hadronic level of the Dirac equation by adding a tensor interaction, motivated by the quark model [44, 45]. In addition, one boson exchange model with underlying approximate SU(3) symmetry in strong interactions, also leads to a weaker spin-orbit forces for the (strange) hyperon-nucleon (YN) than that for the nucleon-nucleon (NN) [46].

In practice, because of its heavy mass ($M_{\Lambda_c^+}^*$), contribution to the single-particle energies from the spin-orbit potential both with or without the inclusion of the correction term, turns out to be even smaller than that for the Λ hypernuclei, and further smaller for the Λ_b hypernuclei [8]. Contribution from the spin-orbit potential with the correction term is typically of order 0.01 MeV, and even the largest case is $\simeq 0.5$ MeV, among all the heavy baryon hypernuclei calculated in this study. This can be understood when one considers the limit, $M_{\Lambda_c^+}^* \rightarrow \infty$ in Eq. (26), where the quantity inside the square brackets varies smoothly from an order of hundred MeV to zero near the surface of the hypernucleus, and the derivative with respect to r is finite. The results for the other heavy baryon hypernuclei are quite similar, and spin-orbit forces give only tiny contributions for the single-particle energies. Thus, the spin-orbit splittings are expected to be small.

3.2 Effects of the Pauli blocking and channel coupling

Below, we briefly explain the effects of the Pauli blocking due to the quark structure, and the channel coupling [9].

Although the present treatment is based on the underlying quark structure of the nucleon and heavy baryons, it is missing an explicit inclusion of the Pauli blocking effect at the quark level among the u and d quarks in the core nucleons and the heavy baryons. For the strange hypernuclei, the effect of the Pauli blocking was included in a specific way at the hadronic level. We follow the treatment of Ref. [9], and include effective Pauli blocking and also the $\Sigma_{c,b}N - \Lambda_{c,b}N$ channel coupling effects, although the channel coupling effect is expected to be smaller than that for the $\Sigma N - \Lambda N$, since the mass difference for the former is larger than the latter. Thus, the channel coupling effect that is included for the Σ_c hypernuclei in the present study should be regarded as the limiting case.

Following Ref. [9], we assume that the Pauli blocking effect is simply proportional to the nucleon baryonic density (or u and d total light quark number density), although one could consider a more complicated density dependence. Then, the Dirac equation for the heavy baryon C , Eq. (5), may be modified by

$$[i\boldsymbol{\gamma} \cdot \boldsymbol{\partial} - M_C^*(\sigma) - (\lambda_C \rho_B(\vec{r}) + g_\omega^C \omega(\vec{r}) + g_\rho I_3^C b(\vec{r}) + eQ_C A(\vec{r}))\gamma_0]\psi_C(\vec{r}) = 0, \quad (28)$$

where, $\rho_B(\vec{r})$ is the baryonic density at the position \vec{r} in the heavy baryon hypernucleus due to the core nucleons, and λ_C is a constant, taken the same value to that determined for the strange hyperon. We note that the Pauli blocking effect associated with the light quarks in the heavy baryon should also lead to some repulsion for the nucleons. Contrary to the comment made in Ref. [9], the actual calculations in this study (and in Ref. [9]) include the effect of the modification made in Eq. (28) in a self-consistent manner. In practice, the above modified Eq. (28) has been inserted again into a system of coupled differential equations for the spherical static (heavy baryon) hypernuclear system, from Eq. (4) to Eq. (18), and calculations are performed again. Thus, the response of the core nucleons due to the modification in Eq. (28) for the heavy baryon, is included.

For the Λ hypernuclei [9] the parameter corresponding to λ_C in Eq. (28) was chosen to reproduce the empirical single particle energy for the $1s_{1/2}$ in ${}_{\Lambda}^{209}\text{Pb}$, -27.0 MeV [48]. The fitted value for the constant was, $\lambda_{\Lambda} = 60.25 \text{ MeV (fm)}^3$. Thus, we use the same value also for the $\Lambda_{c,b}$, i.e., $\lambda_{\Lambda_{c,b}} = 60.25 \text{ MeV (fm)}^3$. For the Σ_c and Ξ_c hypernuclei, we can deduce the constants $\lambda_{\Sigma_c, \Xi_c}$, corresponding to the effective Pauli blocking effect as, $\lambda_{\Sigma_c} = \lambda_{\Lambda_c}$, and $\lambda_{\Xi_c} = \frac{1}{2}\lambda_{\Lambda_c}$, by counting the total number of u and d quarks in the heavy baryons.

One may regard that this fitted value includes also the attractive $\Lambda_{c,b}N \rightarrow \Sigma_{c,b}N$ channel coupling effect for the $\Lambda_{c,b}$ single-particle energies, since the value fitted for the Λ hypernuclei includes the experimentally observed effect of the $\Lambda N \rightarrow \Sigma N$ channel coupling. As for the $\Sigma_c N \rightarrow \Lambda_c N$ channel coupling effect, it must be included in addition to reproduce the relative repulsive energy shift in the single-particle energies for the Σ_c hypernuclei, as was done for the Σ hypernuclei.

The $\Sigma N - \Lambda N$ channel coupling was estimated using the Nijmegen potential in Ref. [9]. The effect for the Σ was included by assuming the same form as that for the effective Pauli blocking via $\lambda_{\Sigma}\rho_B(r)$, and adjusted the parameter, $\lambda_{\Sigma} = \lambda_{\Lambda} \rightarrow \tilde{\lambda}_{\Sigma} \neq \lambda_{\Sigma}$, to reproduce this difference in the single-particle energy for the $1s_{1/2}$ in ${}_{\Sigma}^{209}\text{Pb}$, namely, $-19.6 = -26.9 (\simeq -27.0) + 7.3 \text{ MeV}$. The value obtained for $\tilde{\lambda}_{\Sigma}$ in this way was, $\tilde{\lambda}_{\Sigma} = 110.6 \text{ MeV (fm)}^3$. Thus, we use the same value, $\tilde{\lambda}_{\Sigma_c} = 110.6 \text{ MeV (fm)}^3$, although the effect is expected to be smaller considering the mass differences, $m_{\Sigma} - m_{\Lambda} \simeq 77 \text{ MeV}$ and $m_{\Sigma_c} - m_{\Lambda_c^+} \simeq 166 \text{ MeV}$ [40]. As for the $\Xi N - \Lambda N$ channel coupling the effect was estimated to be negligible in Ref. [9], and we also neglect the effect of channel coupling on Ξ_c in this study.

4 Results for heavy baryon hypernuclei

Before presenting the results, we summarize in Table 3 the parameters at the hadronic level fixed by the saturation properties of symmetric nuclear matter. Concerning the parameters for the σ field, we note that the properties of nuclear matter only fix the ratio, (g_σ/m_σ) , with a chosen value, $m_\sigma = 550$ MeV. Keeping this ratio to be a constant, the value $m_\sigma = 418$ MeV for finite nuclei (hypernuclei) is obtained by fitting the r.m.s. charge radius of ^{40}Ca to the experimental value, $r_{\text{ch}}(^{40}\text{Ca}) = 3.48$ fm [12]. (See also Section 2.1 for the value of g_σ in nuclear matter.)

Table 3: Parameters at the hadronic level for finite nuclei [12].

field	mass (MeV)	$g^2/4\pi (e^2/4\pi)$
σ	418	3.12
ω	783	5.31
ρ	770	6.93
A	0	1/137.036

First, in Tables 4 and 5, we summarize the calculated single-particle energies for $^{17}_j\text{O}$, $^{41}_j\text{Ca}$, $^{49}_j\text{Ca}$, $^{91}_j\text{Zr}$ and $^{209}_j\text{Pb}$ ($j = \Lambda, \Lambda_c^+, \Sigma_c^{0,+}, \Sigma_c^{++}, \Xi_c^{0,+}, \Lambda_b$) hypernuclei, together with the experimental data [47, 48] for the Λ hypernuclei. The results for the Λ_c^+ and Λ_b , and Λ hypernuclei are taken from Refs. [8], and [9], respectively for comparison. In the calculation, we have searched for the single-particle states up to the same highest state as that of the core neutrons in each hypernucleus, since the deeper levels are usually easier to observe in experiment.

After a first look at the results shown in Tables 4 and 5 we notice:

1. Σ_c^{++} and Ξ_c^+ hypernuclei are very unlikely to be formed in usual circumstances. Solid conclusions may not be drawn about $^{49}_{\Sigma_c^{++}, \Xi_c^+}\text{Ca}$. Although results imply the formations of these hypernuclei, those numbers may be regarded within the uncertainties of the model and the approximations made in the calculation. Only a major alteration of the parameters may yield such bound hypernuclei.
2. Σ_c^0 and Σ_c^+ hypernuclei may have some possibilities to be formed. However, due to a peculiar feature that the correct $1s_{1/2}$ state is not found in $^{17}_{\Sigma_c^0}\text{O}$, $^{49}_{\Sigma_c^0}\text{Ca}$ and $^{91}_{\Sigma_c^0}\text{Zr}$, one needs some caution to take this statement naively. (Discussions on this matter will be made later in detail.) A calculational modification could increase confidence in predicting such hypernuclei.
3. Λ_c^+, Ξ_c^0 and Λ_b hypernuclei are expected to be formed quite likely in a realistic situation. However, for the Λ_b hypernuclei, it will be very difficult to achieve such a resolution to distinguish the states experimentally. The question of experimental observation is not tackled realistically.
4. The Coulomb force plays a crucial role in forming (unforming) hypernuclei, by comparing the single-particle energies among/between the members within each multiplet, $(\Lambda, \Lambda_c^+, \Lambda_b)$, $(\Sigma_c^0, \Sigma_c^+, \Sigma_c^{++})$, and (Ξ_c^0, Ξ_c^+) hypernuclei.

Table 4: Single-particle energies (in MeV) for $^{17}_j\text{O}$, $^{41}_j\text{Ca}$ and $^{49}_j\text{Ca}$ ($j = \Lambda, \Lambda_c^+, \Sigma_c, \Xi_c, \Lambda_b$). Results for Λ_c^+ and Λ_b , and Λ hypernuclei are taken from Refs. [8], and [9], respectively. Experimental data are taken from Ref. [47]. Spin-orbit splittings for the Λ hypernuclei are not well determined by the experiments.

	$^{16}_\Lambda\text{O}$ (Expt.)	$^{17}_\Lambda\text{O}$	$^{17}_{\Lambda_c^+}\text{O}$	$^{17}_{\Sigma_c^0}\text{O}$	$^{17}_{\Sigma_c^+}\text{O}$	$^{17}_{\Sigma_c^{++}}\text{O}$	$^{17}_{\Xi_c^0}\text{O}$	$^{17}_{\Xi_c^+}\text{O}$	$^{17}_{\Lambda_b}\text{O}$
$1s_{1/2}$	-12.5	-14.1	-12.8	—	-7.5	—	-7.9	-2.1	-19.6
$1p_{3/2}$	-2.5 (1p)	-5.1	-7.3	-10.7	-4.0	—	-3.5	—	-16.5
$1p_{1/2}$	-2.5 (1p)	-5.0	-7.3	-10.2	-3.6	—	-3.5	—	-16.5
	$^{40}_\Lambda\text{Ca}$ (Expt.)	$^{41}_\Lambda\text{Ca}$	$^{41}_{\Lambda_c^+}\text{Ca}$	$^{41}_{\Sigma_c^0}\text{Ca}$	$^{41}_{\Sigma_c^+}\text{Ca}$	$^{41}_{\Sigma_c^{++}}\text{Ca}$	$^{41}_{\Xi_c^0}\text{Ca}$	$^{41}_{\Xi_c^+}\text{Ca}$	$^{41}_{\Lambda_b}\text{Ca}$
$1s_{1/2}$	-20.0	-19.5	-12.8	-16.3	-6.3	—	-9.9	-1.0	-23.0
$1p_{3/2}$	-12.0 (1p)	-12.3	-9.2	-13.2	-4.1	—	-6.7	—	-20.9
$1p_{1/2}$	-12.0 (1p)	-12.3	-9.1	-12.9	-3.8	—	-6.7	—	-20.9
$1d_{5/2}$		-4.7	-4.8	-9.9	—	—	-3.3	—	-18.4
$2s_{1/2}$		-3.5	-3.4	-9.3	—	—	-2.8	—	-17.4
$1d_{3/2}$		-4.6	-4.8	-9.4	—	—	-3.3	—	-18.4
	—	$^{49}_\Lambda\text{Ca}$	$^{49}_{\Lambda_c^+}\text{Ca}$	$^{49}_{\Sigma_c^0}\text{Ca}$	$^{49}_{\Sigma_c^+}\text{Ca}$	$^{49}_{\Sigma_c^{++}}\text{Ca}$	$^{49}_{\Xi_c^0}\text{Ca}$	$^{49}_{\Xi_c^+}\text{Ca}$	$^{49}_{\Lambda_b}\text{Ca}$
$1s_{1/2}$		-21.0	-14.3	—	-7.4	-5.0	-7.8	-5.1	-24.4
$1p_{3/2}$		-13.9	-10.6	-7.2	-5.1	-3.4	-4.1	-2.8	-22.2
$1p_{1/2}$		-13.8	-10.6	-7.0	-4.9	-3.2	-4.1	-2.8	-22.2
$1d_{5/2}$		-6.5	-6.5	-4.0	-2.3	—	-0.9	—	-19.5
$2s_{1/2}$		-5.4	-5.3	-4.9	—	—	-1.5	—	-18.8
$1d_{3/2}$		-6.4	-6.4	-3.6	-1.9	—	-1.0	—	-19.5
$1f_{7/2}$		—	-2.0	—	—	—	—	—	-16.8

Table 5: Single-particle energies (in MeV) for ${}^{91}_j\text{Zr}$ and ${}^{208}_j\text{Pb}$ ($j = \Lambda, \Lambda_c^+, \Sigma_c, \Xi_c, \Lambda_b$). Results for Λ_c^+ and Λ_b , and Λ hypernuclei are taken from Refs. [8], and [9], respectively. Experimental data are taken from Ref. [48]. Spin-orbit splittings for the Λ hypernuclei are not well determined by the experiments. The values given inside the brackets for ${}^{91}_{\Sigma_c^0}\text{Zr}$ are those obtained by switching off both the Pauli blocking and the channel coupling effects simultaneously by setting $\tilde{\lambda}_{\Sigma_c} = 0$.

	${}^{89}_{\Lambda}\text{Yb}$ (Expt.)	${}^{91}_{\Lambda}\text{Zr}$	${}^{91}_{\Lambda_c^+}\text{Zr}$	${}^{91}_{\Sigma_c^0}\text{Zr}$	${}^{91}_{\Sigma_c^+}\text{Zr}$	${}^{91}_{\Sigma_c^{++}}\text{Zr}$	${}^{91}_{\Xi_c^0}\text{Zr}$	${}^{91}_{\Xi_c^+}\text{Zr}$	${}^{91}_{\Lambda_b}\text{Zr}$
$1s_{1/2}$	-22.5	-23.9	-10.8	— (—)	-3.7	—	-9.3	—	-25.7
$1p_{3/2}$	-16.0 (1 <i>p</i>)	-18.4	-8.7	-10.2 (-26.5)	-2.3	—	-6.6	—	-24.2
$1p_{1/2}$	-16.0 (1 <i>p</i>)	-18.4	-8.7	-10.1 (-26.4)	-2.1	—	-6.7	—	-24.2
$1d_{5/2}$	-9.0 (1 <i>d</i>)	-12.3	-5.8	-7.6 (-21.8)	—	—	-4.0	—	-22.4
$2s_{1/2}$		-10.8	-3.9	-8.1 (-23.0)	—	—	-3.9	—	-21.6
$1d_{3/2}$	-9.0 (1 <i>d</i>)	-12.3	-5.8	-7.3 (-21.6)	—	—	-4.0	—	-22.4
$1f_{7/2}$	-2.0 (1 <i>f</i>)	-5.9	-2.4	-5.1 (-17.1)	—	—	-1.3	—	-20.4
$2p_{3/2}$		-4.2	—	-5.0 (-16.5)	—	—	-1.3	—	-19.5
$1f_{5/2}$	-2.0 (1 <i>f</i>)	-5.8	-2.4	-4.7 (-16.8)	—	—	-1.4	—	-20.4
$2p_{1/2}$		-4.1	—	-4.9 (-16.3)	—	—	-1.3	—	-19.5
$1g_{9/2}$		—	—	-2.4 (-12.4)	—	—	—	—	-18.1
	${}^{208}_{\Lambda}\text{Pb}$ (Expt.)	${}^{209}_{\Lambda}\text{Pb}$	${}^{209}_{\Lambda_c^+}\text{Pb}$	${}^{209}_{\Sigma_c^0}\text{Pb}$	${}^{209}_{\Sigma_c^+}\text{Pb}$	${}^{209}_{\Sigma_c^{++}}\text{Pb}$	${}^{209}_{\Xi_c^0}\text{Pb}$	${}^{209}_{\Xi_c^+}\text{Pb}$	${}^{209}_{\Lambda_b}\text{Pb}$
$1s_{1/2}$	-27.0	-27.0	-5.2	-7.5	—	—	-6.7	—	-27.4
$1p_{3/2}$	-22.0 (1 <i>p</i>)	-23.4	-4.1	-6.6	—	—	-5.4	—	-26.6
$1p_{1/2}$	-22.0 (1 <i>p</i>)	-23.4	-4.0	-6.5	—	—	-5.5	—	-26.6
$1d_{5/2}$	-17.0 (1 <i>d</i>)	-19.1	-2.4	-5.3	—	—	-3.9	—	-25.4
$2s_{1/2}$		-17.6	—	—	—	—	-3.3	—	-24.7
$1d_{3/2}$	-17.0 (1 <i>d</i>)	-19.1	-2.4	-5.1	—	—	-4.0	—	-25.4
$1f_{7/2}$	-12.0 (1 <i>f</i>)	-14.4	—	-3.8	—	—	-2.2	—	-24.1
$2p_{3/2}$		-12.4	—	—	—	—	-1.4	—	-23.2
$1f_{5/2}$	-12.0 (1 <i>f</i>)	-14.3	—	-3.5	—	—	-2.3	—	-24.1
$2p_{1/2}$		-12.4	—	—	—	—	-1.5	—	-23.2
$1g_{9/2}$	-7.0 (1 <i>g</i>)	-9.3	—	-2.1	—	—	—	—	-22.6
$1g_{7/2}$	-7.0 (1 <i>g</i>)	-9.2	—	-1.8	—	—	—	—	-22.6
$1h_{11/2}$		-3.9	—	—	—	—	—	—	-21.0
$2d_{5/2}$		-7.0	—	—	—	—	—	—	-21.7
$2d_{3/2}$		-7.0	—	—	—	—	—	—	-21.7
$1h_{9/2}$		-3.8	—	—	—	—	—	—	-21.0
$3s_{1/2}$		-6.1	—	—	—	—	—	—	-21.3
$2f_{7/2}$		-1.7	—	—	—	—	—	—	-20.1
$3p_{3/2}$		-1.0	—	—	—	—	—	—	-19.6
$2f_{5/2}$		-1.7	—	—	—	—	—	—	-20.1
$3p_{1/2}$		-1.0	—	—	—	—	—	—	-19.6
$1i_{13/2}$		—	—	—	—	—	—	—	-19.3

We discuss below in detail the Σ_c^0 hypernuclei single-particle energies, which have a peculiar feature. In some of the hypernuclei calculated, the $1s_{1/2}$ state could not be found in the following sense. We have searched for the $1s_{1/2}$ state by varying matching point to get the eigenenergy and the corresponding eigen wave function for the Σ_c^0 in steps 0.1 fm, from 0.2 fm to 5.0 fm from the center of the hypernucleus. However, always a proper level with lower energy than those of the $1p_{1/2}$, $1p_{3/2}$ and $2s_{1/2}$ states could not be found, although a smaller matching point than that for the $2s_{1/2}$ state and the Dirac's $\kappa = -1$ necessary to obtain the correct $1s_{1/2}$ wave function were input. In such a case, the single-particle energy level became equal or higher than that of the $2s_{1/2}$ state, which is also above the levels of the $1p_{1/2}$ and $1p_{3/2}$ states. In the search procedure, we always checked that the core nucleon single-particle energy levels are in correct order. But, whenever we get the lower single-particle energy level for the $1s_{1/2}$ state than those for the $1p_{1/2}$, $1p_{3/2}$ and $2s_{1/2}$ states, the core neutron $1s_{1/2}$ energy level jumped to become equal or larger than that of the $2s_{1/2}$, and we discarded the results in such cases. In this manner, the $1s_{1/2}$ state in $^{17}_{\Sigma_c^0}\text{O}$, $^{49}_{\Sigma_c^0}\text{Ca}$ and $^{91}_{\Sigma_c^0}\text{Zr}$ could not be found.

To get greater insight as to what happens, as an example, we show in Figs. 2 and 3 the potential strengths and baryon density (together with the baryon density of nucleons), respectively for Σ_c^0 in $^{91}_{\Sigma_c^0}\text{Zr}$, giving incorrect-" $1s_{1/2}(?)$ " (notation used in the figures) and correct- $2s_{1/2}$ states. "Pa.+CC." stands for potential for the effective Pauli blocking plus the channel coupling effects. By the terminology, incorrect-" $1s_{1/2}(?)$ " state, we mean by that the obtained solution is incorrect, since both the single-particle energy for the Σ_c^0 and the core nucleon energy levels are incorrect. In this case, the obtained single-particle energies for the Σ_c^0 are, -7.4 and -8.1 MeV, respectively for the " $1s_{1/2}(?)$ " and $2s_{1/2}$ states. Looking at the potential strengths in Fig. 2, the difference between the two states are only slight, and nearly indistinguishable. However, looking at the Σ_c^0 baryon density (scaled by a factor 5) in Fig. 3, it is clear that both solutions have two nodes, thus actually they are $2s_{1/2}$ states. The Σ_c^0 density distributions are very different, because the core nucleon density distributions (particularly around 3 fm from the center of the hypernucleus) are appreciably different due to the incorrect core nucleon single-particle energy levels. The main difference in the calculation of the Σ_c hypernuclei from that of the Σ hypernuclei is the bare (effective) mass, where mass of the Σ_c is much larger, and the wave function (if obtained) for the $1s_{1/2}$ is expected to be localized considerably in the central region of each Σ_c hypernucleus when the isospin dependent strong interaction and Coulomb forces are neglected. This may also be a consequence of an interplay between the isospin dependent force for the Σ_c^0 (the isospin third component is -1), and baryonic density in the central region. To test this we have repeated the calculation for $^{91}_{\Sigma_c^0}\text{Zr}$ single-particle energies by switching off both the Pauli blocking and the channel coupling effects simultaneously by setting $\tilde{\lambda}_{\Sigma_c} = 0$. The results are shown inside the brackets in Table 5. First, the energy levels from $1p_{3/2}$ to $1g_{9/2}$ states seem to be correct. But again the correct $1s_{1/2}$ state solution is not found, in the sense that the lowest single-particle energy for s -state obtained is -23.0 MeV, and the corresponding wave function has two nodes ($2s_{1/2}$ state). Then, we have looked into the behavior of ρ meson field, particularly near the center of $^{91}_{\Sigma_c^0}\text{Zr}$, which may show some hints. Indeed, we have found following, different and distinct behaviors of the ρ meson field between the $2s_{1/2}$ state and that for the other (non- s) states:

- For all the non- s states calculated, ρ meson field is repulsive and varies in the range $+2 \sim +5$ MeV up to ~ 4 fm from the center of $^{91}_{\Sigma_c^0}\text{Zr}$, and gradually dies out towards the surface.

- For the $2s_{1/2}$ state, it is strong *attraction* relative to that for the non- s states, $-28 \sim -20$ MeV up to ~ 0.4 fm from the center of ${}^{91}_{\Sigma_c^0}\text{Zr}$, and changes to *repulsion* around ~ 1 fm, to become maximum of $\sim +7$ MeV around 4 fm from the center, and similarly for the other states, gradually dies out towards the surface.

This implies that the $1s_{1/2}$ state would need much stronger attractive ρ meson field than that for the $2s_{1/2}$ state to exist near the center of ${}^{91}_{\Sigma_c^0}\text{Zr}$. However, such a case would certainly disturb the core neutrons which are bound deeply nearer to the center of ${}^{91}_{\Sigma_c^0}\text{Zr}$, and result in giving incorrect core neutron energy levels as we have to discard such a solution observed. Therefore we discard such a solution. Thus, we would conclude that the peculiar feature of not finding the correct $1s_{1/2}$ state in ${}^{91}_{\Sigma_c^0}\text{Zr}$ (and probably also for ${}^{49}_{\Sigma_c^0}\text{Ca}$) is due to the behavior of the isospin-dependent ρ meson field at very near the center of ${}^{91}_{\Sigma_c^0}\text{Zr}$. If one ignores the incorrect energy levels of the core neutrons, one would get a solution and regard it as a " $1s_{1/2}$ " state, which is not correct in reality. As we will discuss later again in case of $1s_{1/2}$ state in ${}^{209}_{\Sigma_c^0}\text{Pb}$, indeed the isospin dependent ρ -meson field is expected to work in a peculiar manner for the Σ_c^0 - $1s_{1/2}$ state in neutron rich Σ_c^0 hypernuclei.

On the other hand, recent experiment [49] suggests that a strongly repulsive Σ -nucleus potential with a non-zero size of the imaginary part is favorable to reproduce the measured spectra for middle and large baryon number hypernuclei. If we wish to be consistent with this result, we need to introduce even stronger repulsive potential, either by the channel coupling effect, or based on the quark model analysis to reproduce the Σ -atom data without resorting to the channel coupling effect [50], for the treatments of both the Σ and Σ_c hypernuclei. In this case, the repulsion should be strong enough so that it entails no bound state for the Σ hypernuclei (and probably also for the Σ_c hypernuclei) in the middle and large baryon number hypernuclei. This will need a more elaborate investigation in the future, using further accumulated experimental data and analyses.

Next, in Figs. 4 and 5 we show the potential strengths for the $1s_{1/2}$ state found in ${}^{41}_j\text{Ca}$ and ${}^{209}_j\text{Pb}$ ($j = \Sigma_c^{0,+}, \Xi_c^0$). Recall that the effects are different for the Λ_c^+ and Σ_c as they are true for the Λ and Σ . As in the limit of nuclear matter in Section 2.2, the scalar and vector potentials for the heavy baryons are also quite similar to the strange hyperons with the same light quark numbers in the corresponding hypernuclei. This feature also holds between the Σ_c and Σ in the corresponding hypernuclei, except for a contributions due to the differences in charges, where the Coulomb force affects the baryon density distributions and then the vector and scalar potentials are also slightly modified. Thus, as far as the total baryon density distributions and the scalar and vector potentials are concerned, among/between the members within each multiplet, $(\Lambda, \Lambda_c^+, \Lambda_b)$, (Σ, Σ_c) and (Ξ, Ξ_c) hypernuclei, they show quite similar features. However, in realistic nuclei, the Coulomb force plays a crucial role as mentioned before, and the single-particle energies thus obtained show very different features within each hypernuclei multiplet. Of course, the mass differences within the multiplet is also the dominant source for the differences in the obtained single-particle energies.

The probability density distributions for the heavy baryons for the $1s_{1/2}$ state, in ${}^{41}_j\text{Ca}$ and ${}^{209}_j\text{Pb}$ ($j = \Sigma_c^{0,+}, \Xi_c^0$), are shown in Fig. 6. (We mention that the wave function for the $1s_{1/2}$ state for ${}^{41}_{\Sigma_c^0}\text{Ca}$ is correct, because it has one node as shown in Fig. 6.) It is interesting to compare the Σ_c^0 and Ξ_c^0 probability density distributions. Due to the Pauli blocking and the channel coupling effects, the probability density distributions for the Σ_c^0 are pushed away from the origin compared to those for the Ξ_c^0 in both ${}^{41}_{\Sigma_c^0}\text{Ca}$ and ${}^{209}_{\Sigma_c^0}\text{Pb}$. In particular, the Σ_c^0 density

distributions in ${}^{209}_{\Sigma_c^0}\text{Pb}$ are really pushed away from the central region, and thus nearly losing the character of a typical $1s_{1/2}$ state wave function. This fact shows that the isospin dependent ρ -meson mean field for the Σ_c^0 $1s_{1/2}$ state in central region of the neutron rich nuclei is very important as discussed before, and that explains why the correct $1s_{1/2}$ state wave functions are not obtained in ${}^{49}_{\Sigma_c^0}\text{Ca}$ and ${}^{91}_{\Sigma_c^0}\text{Zr}$, where the (isospin asymmetric) baryon density distributions in central region of these nuclei are expected to be larger than those for the ${}^{209}_{\Sigma_c^0}\text{Pb}$ as in the case of normal nuclei. (In the case of ${}^{17}_{\Sigma_c^0}\text{O}$, we expect that the size of the nucleus is much smaller and Σ_c^0 feels more sensitively the isospin dependent ρ -meson mean field, due to the higher baryon density and the limitation of the mean field approximation than those for the ${}^{209}_{\Sigma_c^0}\text{Pb}$.) On the contrary, it is rather surprising that the Ξ_c^0 probability density distributions are higher and localized in the central region than those for the $\Sigma_c^{0,+}$, although one can naively expect that they have an opposite characteristic, because of the smaller scalar attractive potential for the Ξ_c^0 . Thus, in the present calculation the effects of the Pauli blocking, and particularly the channel coupling, play an important role for these different features. Then, we must be careful in drawing any definite conclusions from the Σ_c^0 and Σ_c^+ probability density distributions.

Finally, we show in Table 6 the calculated binding energy per baryon, $-E/A$, r.m.s charge radius, r_{ch} , and r.m.s radii of the heavy baryon (also Λ), neutron and proton distributions, r_j , r_n and r_p , respectively. The results listed in Table 6 are calculated with the $1s_{1/2}$ heavy baryon configuration for all cases. At a first glance, it is very clear that the r.m.s radius for the Λ_b is very small compared to those for other baryons within the same baryon number hypernuclei as one would expect, due to heavy mass. On the other hand, r_{ch} and/or r_p for the Λ_b hypernuclei are usually the largest in the all hypernuclei calculated. This implies that the protons in the core nucleus are relatively more pushed away compared to the other hypernuclei, although such feature is not seen for r_n . The radii, r_{ch} , r_n and r_p , may be grouped in similar magnitudes for all heavy baryon hypernuclei and Λ hypernuclei within the same baryon number multiplet (${}^{41}_j\text{Ca}$ and ${}^{49}_j\text{Ca}$ in Table 6 may be grouped together), reflecting the fact that the effect of the embedded baryon on these quantities are of order, $\simeq M_{C,\Lambda}/[(A-1)M_N + M_{C,\Lambda}]$. As for the binding energy per baryon, the energy of Λ_b hypernuclei is usually the largest among the same baryon number hypernuclei. One of the largest contributions for this is the single-particle energy of the $1s_{1/2}$ state, even after dividing by the total baryon number.

5 Summary and discussion

In summary, we have completed systematic studies of the Λ_c^+ , Σ_c , Ξ_c and Λ_b hypernuclei in the QMC model, extending the study made for strange hypernuclei [9]. The spin-orbit potentials for the heavy baryon hypernuclei are negligible for the single-particle energies, because of their heavy masses. Our results suggest that the formation of Λ_c^+ , Ξ_c^0 and Λ_b hypernuclei is expected to be quite likely, while that of the Σ_c^{++} and Ξ_c^+ is unlikely. For the Σ_c^0 and Σ_c^+ hypernuclei, although there may be some possibilities to be formed, it is difficult to draw a solid conclusion in view of the uncertainties in the model and approximations made in the calculations.

For the Σ_c and Ξ_c hypernuclei, the Coulomb force is crucial in the possibility to form the hypernuclei, in particular for the $\Sigma_c^{+,++}$ hypernuclei. The results for the Σ_c hypernuclei imply that the phenomenologically introduced channel coupling effects may be overestimated when using the same strength as that for the Σ hypernuclei. Thus, we need to investigate further how such effects can be included consistently with the underlying quark structure. In this sense,

Table 6: Binding energy per baryon, $-E/A$ (in MeV), r.m.s charge radius, r_{ch} , and r.m.s radii of the Λ and heavy baryons, r_j , neutron, r_n , and proton, r_p (in fm) for ${}^{17}_j\text{O}$, ${}^{41}_j\text{Ca}$, ${}^{49}_j\text{Ca}$, ${}^{91}_j\text{Zr}$ and ${}^{209}_j\text{Pb}$ ($j = \Lambda, \Lambda_c^+, \Sigma_c, \Xi_c, \Lambda_b$). The configurations of the Λ and heavy baryon j , are $1s_{1/2}$ for all hypernuclei.

hypernuclei	$-E/A$	r_{ch}	r_j	r_n	r_p
${}^{17}_\Lambda\text{O}$	6.37	2.84	2.49	2.59	2.72
${}^{17}_{\Lambda^+}\text{O}$	6.42	2.85	2.19	2.58	2.73
${}^{17}_{\Sigma_c^+}\text{O}$	6.10	2.83	2.57	2.60	2.71
${}^{17}_{\Xi_c^0}\text{O}$	6.01	2.81	2.34	2.61	2.69
${}^{17}_{\Xi_c^+}\text{O}$	5.84	2.81	2.70	2.61	2.69
${}^{17}_{\Lambda_b}\text{O}$	6.69	2.87	1.81	2.57	2.75
${}^{41}_\Lambda\text{Ca}$	7.58	3.51	2.81	3.31	3.42
${}^{41}_{\Lambda^+}\text{Ca}$	7.58	3.51	2.66	3.31	3.42
${}^{41}_{\Sigma_c^+}\text{Ca}$	7.54	3.51	2.79	3.31	3.42
${}^{41}_{\Sigma_c^0}\text{Ca}$	7.42	3.50	3.21	3.31	3.41
${}^{41}_{\Xi_c^0}\text{Ca}$	7.43	3.49	2.76	3.32	3.40
${}^{41}_{\Xi_c^+}\text{Ca}$	7.32	3.49	3.11	3.32	3.39
${}^{41}_{\Lambda_b}\text{Ca}$	7.72	3.53	2.22	3.30	3.43
${}^{49}_\Lambda\text{Ca}$	7.58	3.54	2.84	3.63	3.45
${}^{49}_{\Lambda^+}\text{Ca}$	7.54	3.54	2.67	3.63	3.45
${}^{49}_{\Sigma_c^+}\text{Ca}$	7.39	3.54	3.17	3.64	3.44
${}^{49}_{\Sigma_c^{++}}\text{Ca}$	6.29	3.57	3.62	3.71	3.47
${}^{49}_{\Xi_c^0}\text{Ca}$	7.34	3.53	2.57	3.65	3.43
${}^{49}_{\Xi_c^+}\text{Ca}$	7.32	3.53	3.19	3.65	3.43
${}^{49}_{\Lambda_b}\text{Ca}$	7.64	3.56	2.16	3.63	3.46
${}^{91}_\Lambda\text{Zr}$	7.95	4.29	3.25	4.29	4.21
${}^{91}_{\Lambda^+}\text{Zr}$	7.85	4.29	3.34	4.30	4.21
${}^{91}_{\Sigma_c^+}\text{Zr}$	7.77	4.29	4.03	4.30	4.21
${}^{91}_{\Xi_c^0}\text{Zr}$	7.78	4.28	3.01	4.30	4.20
${}^{91}_{\Lambda_b}\text{Zr}$	7.93	4.30	2.63	4.29	4.22
${}^{209}_\Lambda\text{Pb}$	7.35	5.49	3.99	5.67	5.43
${}^{209}_{\Lambda^+}\text{Pb}$	7.26	5.49	4.74	5.68	5.43
${}^{209}_{\Sigma_c^0}\text{Pb}$	6.95	5.51	4.88	5.70	5.45
${}^{209}_{\Xi_c^0}\text{Pb}$	7.24	5.49	4.44	5.68	5.43
${}^{209}_{\Lambda_b}\text{Pb}$	7.48	5.49	3.45	5.66	5.43

some of the results for the Σ_c hypernuclei need to be taken with caution.

Although there can be numerous speculations on the implications of the present results we would like to emphasize that our calculations indicate that the Λ_c^+ , Ξ_c^0 , and Λ_b hypernuclei would exist in realistic experimental conditions, but there may be lesser possibilities for the Σ_c^0 and Σ_c^+ hypernuclei. Furthermore, it is very unlikely that the Σ_c^{++} and Ξ_c^+ hypernuclei will be formed. Experiments at facilities like JHF would provide quantitative input to gain a better understanding of the interactions of heavy baryons with nuclear matter. Experiments at colliders such as RHIC, LHC and Fermilab could provide additional data to establish the formation and decay of such heavy baryon hypernuclei. A combination of these data inputs and a careful analysis, with the present calculations being considered as a first step, would give a valuable information about the physical implications for the presence of heavy quarks in finite nuclei or dense nuclear matter. Furthermore, the experiments would indicate certainly the shortcomings of the QMC model and in addition would provide a guide to a proper and consistent model to treat baryons with heavy quarks in finite nuclei or nuclear matter. Eventually we hope that these results will have important implications for studies in astrophysics of neutron stars and nuclear matter at very high densities.

As for the other aspects of interests for the properties of heavy baryons in nuclear medium, additional studies are needed to investigate the semi-leptonic weak decay of Λ_c^+ , Σ_c , Ξ_c and Λ_b hyperons in nuclear medium. This will provide information on the weak current form factors of heavy baryons in nuclear medium, whether or not the axial coupling constant of such heavy system will be modified appreciably, as is the case implied for the quenching g_A of nucleon, possibly due to the internal structure change of the heavy baryon in medium [51]. To determine the role of Pauli blocking and density in influencing the decay rates as compared to the free heavy baryons would be highly desirable. Such studies can provide important information on the hadronization of the quark-gluon plasma and the transport of hadrons in nuclear matter at high density. Will the high density lead to a slower decay and a higher probability to survive its passage through the material? At present the study of the presence of heavy baryons in finite nuclei and/or nuclear matter is in its infancy. Careful investigations, both theoretical and experimental, would lead to a much better understanding of the properties of heavy quarks and/or heavy baryons in finite nuclei and nuclear matter.

Acknowledgment

The authors would like to thank Prof. A.W. Thomas for the hospitality at CSSM, Adelaide, where this work was initiated. KT acknowledges support and warm hospitality at University of Alberta, where main part of the calculation was completed. He also would like to thank Profs. F.S. Navarra and M. Nielsen for making it possible to use the computer facility in Uni. São Paulo to perform new calculations. KT was supported by the Forschungszentrum-Jülich, contract No. 41445282 (COSY-058), and is supported by FAPESP contract 2003/06814-8. The work of FK is supported by NSERCC.

References

- [1] Guichon P A M 1989 *Phys. Lett.* **B 200** 235
- [2] Tsushima K and Khanna F C 2003 *Phys. Lett.* **B 552** 138

- [3] Tyapkin A A 1976 *Sov. J. Nucl. Phys.* **22** 89
- [4] Dover C B and Kahana S H 1977 *Phys. Rev. Lett.* **39** 1506
- [5] Gibson B F, Dover C B, Bhamati G and Lehman D R 1982 *Phys. Rev. C* **27** 2085
- [6] Bando H and Bando M 1982 *Phys. Lett. B* **109** 164; Bando H and Nagata S 1983 *Prog. Theor. Phys.* **69** 557
- [7] Bressani T and Iazzi F 1989 *Nuovo. Cim.* **102 A** 597; Buyatov S A, Lyukov V V, Strakov N I and Tsarev V A 1991 *Nuovo. Cim.* **104 A** 1361
- [8] Tsushima K and Khanna F C 2003 *Phys. Rev. C* **67** 015211; 2003 *Prog. Theor. Phys. Suppl.* **149** 169
- [9] Tsushima K, Saito K, Haidenbauer J and Thomas A W 1998 *Nucl. Phys. A* **630** 691; Tsushima K, Saito K and Thomas A W 1997 *Phys. Lett. B* **411** 9; 1998 (E) *Phys. Lett. B* **421** 413
- [10] For example, the proceedings of Joint CSSM/JHF/NITP Workshop on Physics at the Japan Hadron Facility, Adelaide, Australia, 14-21 Mar 2002, p. 303, Eds. Guzey V, Kizilersü A, Nagae T and Thomas A W *World Scientific*
- [11] Guichon P A M, Saito K, Rodionov E N, Thomas A W 1996 *Nucl. Phys. A* **601** 349; Guichon P A M, Saito K and Thomas A W 1997 *Austral. J. Phys.* **50** 115
- [12] Saito K, Tsushima K and Thomas A W 1996 *Nucl. Phys. A* **609** 339
- [13] Saito K and Thomas A W 1994 *Phys. Lett. B* **327** 9; 1995 *Phys. Rev. C* **51** 2757; 1995 *Phys. Rev. C* **52** 2789
- [14] Tsushima K, Saito K and Thomas A W 1999 *Phys. Lett. B* **465** 27; Lu D H *et al* 1998 *Phys. Lett. B* **417**; 1998 *Phys. Lett. B* **417** 217; 1998 *Phys. Lett. B* **441** 27; 1998 *Nucl. Phys. A* **634** 443; 1999 *Phys. Rev. C* **60** 068201; Steffens F M *et al* 1999 *Phys. Lett. B* **447** 233; Saito K, Tsushima K and Thomas A W 1999 *Phys. Lett. B* **460** 17; 1999 *Phys. Lett. B* **465** 27; Tsushima K, Saito K and Thomas A W 1999 *Phys. Lett. B* **465** 36; Tsushima K, in the proceedings, *ISHEP 98*, Dubna, Russia, 17-22 Aug 1998, nucl-th/9811063; *Nucl. Phys. A* **670** 198c; Tsushima K *et al* 2001 *Nucl. Phys. A* **680** 280c; Melnitchouk W, Tsushima K and Thomas A W 2002 *Eur. Phys. J. A* **14** 105; Tsushima K 2002 in the proceedings of Joint CSSM/JHF/NITP Workshop on Physics at the Japan Hadron Facility, Adelaide, Australia, 14-21 Mar 2002, p. 303, Eds. Guzey V, Kizilersü A, Nagae T and Thomas A W *World Scientific*
- [15] Tsushima K, Lu D H, Thomas A W and Saito K 1998 *Phys. Lett. B* **443** 26
- [16] Tsushima K, Lu D H, Thomas A W, Saito K and Landau R H 1999 *Phys. Rev. C* **59** 2824
- [17] For recent applications of QMC, e.g., Tsushima K *et al* 2003 nucl-th/0301078, to be published in the Proceedings of the Joint JLab-UGA Workshop on “Modern Sub-Nuclear Physics and JLab Experiments”, Sep. 13, 2002, Athens Georgia, USA

- [18] Sibirtsev A, Tsushima K, Saito K and Thomas A W, 2000 *Phys. Lett.* **B 484** 23
- [19] Sibirtsev A, Tsushima K and Thomas A W 1999 *Eur. Phys. J.* **A 6** 351
- [20] Tsushima K, Saito K, Thomas A W and Wright S V 1998 *Phys. Lett.* **B 429** 239; 1998 (E) *Phys. Lett.* **B 436** 453; Tsushima K, Sibirtsev A and Thomas A W 2000 *Phys. Rev.* **C 62** 064904; 2001 *J. Phys.* **G 27** 349
- [21] Blunden P G and Miller G A 1996 *Phys. Rev.* **C 54** 359
- [22] Jin X and Jennings B K 1996 *Phys. Lett.* **B 374** 13; 1996 *Phys. Rev.* **C 54** 1427; *Phys. Rev.* **C 55** 1567
- [23] Fleck S *et al* 1990 *Nucl. Phys.* **A 510** 731; Mishra V K *et al* 1992 *Phys. Rev.* **C 46** 1143; Banerjee M K 1992 *Phys. Rev.* **C 45** 1359; Naar E and Birse M C 1993 *J. Phys.* **G 19** 555
- [24] Hayashigaki A 1999 *Prog. Theor. Phys.* **101** 923
- [25] Klingl F, Kim S, Lee S H, Morath P and Weise W, 1999 *Phys. Rev. Lett.* **82** 3396
- [26] Hayashigaki A 2000 *Phys. Lett.* **B 487** 96
- [27] Malov S *et al* 2000 *Phys. Rev.* **C 62** 057302 Dieterich S *et al* 2001 *Phys. Lett.* **B 500** 47; Ransome R D 2002 *Nucl. Phys.* **A 699** 360c; Strauch S *et al* 2003 *Phys. Rev. Lett.* **91** 052301; Strauch S (E93-049 Coll.) 2003 nucl-ex/0308026
- [28] Saito K, Tsushima K and Thomas A W 1997 *Phys. Rev.* **C 55** 2637; 1997 *Phys. Rev.* **C 56** 566
- [29] Krein G, Thomas A W and Tsushima K 1999 *Nucl. Phys.* **A 650** 313
- [30] Sawafta R I for the E887 and E905 Collaborations 1998 *Nucl. Phys.* **A 639** 103c, and references therein; Bart S *et al* 1999 *Phys. Rev. Lett.* **83** 5238
- [31] Harada T 1998 *Phys. Rev. Lett.* **81** 5287
- [32] Ahn J K *et al* 2001 *Phys. Rev. Lett.* **87** 132504; Takahashi H *et al* 2001 *Phys. Rev. Lett.* **87** 212502
- [33] Saito K and Tsushima K 2001 *Prog. Theor. Phys.* **105** 373
- [34] Walecka J D 1974 *Ann. Phys. (N.Y.)* **83** 491; Serot B D and Walecka J D 1986 *Adv. Nucl. Phys.* **16** 1
- [35] Furnstahl R J and Serot B D 1987 *Nucl. Phys.* **A 468** 539
- [36] Cohen J 1993 *Phys. Rev.* **C 48** 1346
- [37] Cohen J and Furnstahl R J 1987 *Phys. Rev.* **C 35** 2231
- [38] Barnett R M *et al* 1996 *Phys. Rev.* **D54** 1
- [39] Groom D E *et al* 2000 *Eur. Phys. J.* **C15** 1

- [40] Hagiwara K *et al* 2002 *Phys. Rev.* **D 66** 010001
- [41] Mareš J and Žofka J 1989 *Z. Phys.* **A 333** 209
- [42] Rufa M, Stöcker H, Reinhard P-G, Maruhn J and Greiner W, 1987 *J. Phys.* **G13** L143
- [43] Cooper E D, Jennings B K and Mareš J 1994 *Nucl. Phys.* **A 580** 419; Mareš J and Jennings B K 1994 *Phys. Rev.* **C 49** 2472; 1995 *Nucl. Phys.* **A 585** 347c; Mareš J, Jennings B K and Cooper E D 1994 *Prog. Theor. Phys. Supp.* **117** 415
- [44] Jennings B K 1990, *Phys. Lett.* **B 246** 325; Chiapparini M, Gattone A O and Jennings B K 1991 *Nucl. Phys.* **A 529** 589
- [45] Cohen J and Weber H J 1991 *Phys. Rev.* **C 44** 1181
- [46] Dover C B and Gal A 1985 *Prog. Part. Nucl. Phys.* **12** 171
- [47] Chrien R E 1988 **A478** 705c
- [48] Ajimura S *et al* 1995 *Nucl. Phys.* **A 585** 173c
- [49] Saha P K *et al* 2004 nucl-ex/0405031
- [50] Mareš J *et al* 1995 *Nucl. Phys.* **A 594** 311
- [51] Lu D H, Thomas A W and Tsushima K 2001 nucl-th/0112001

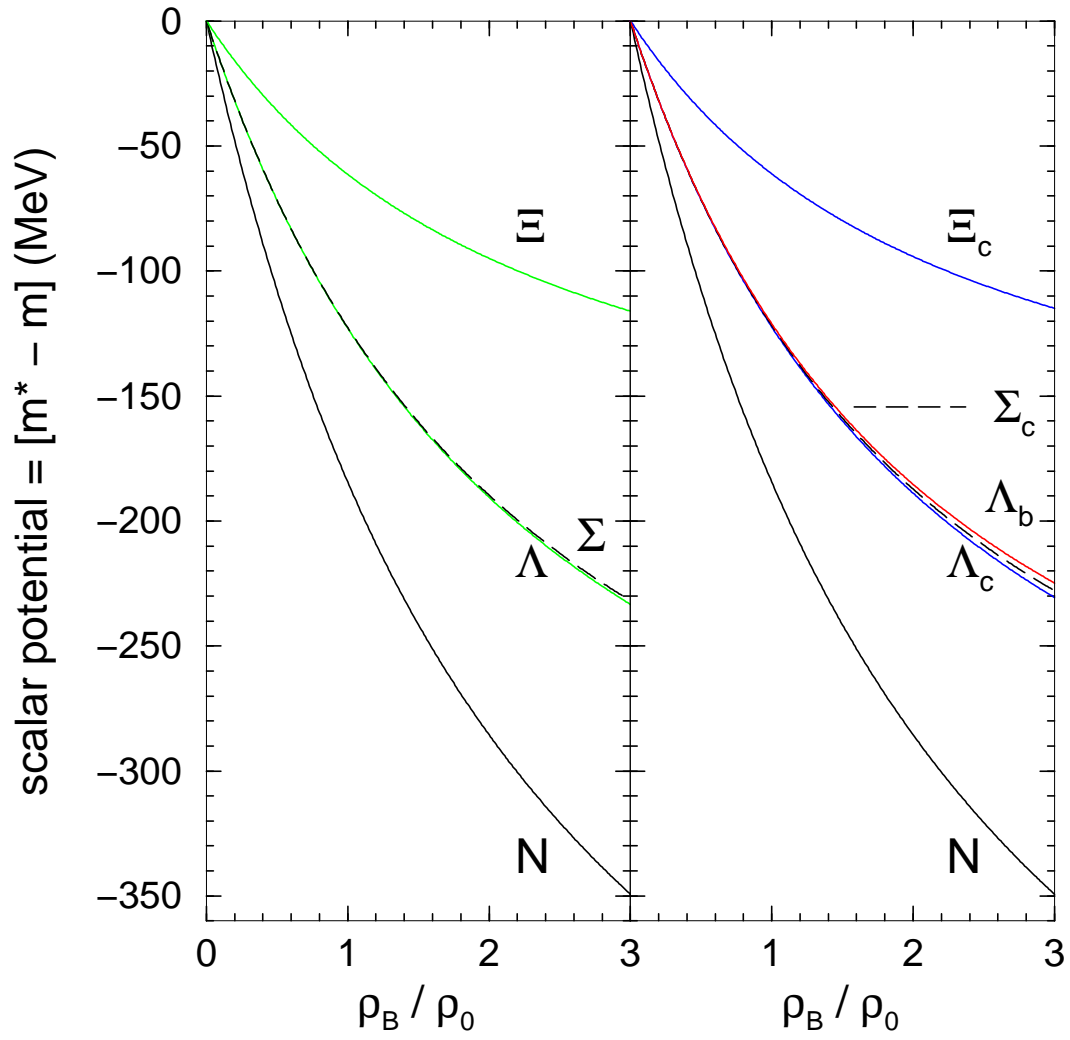


Figure 1: Scalar potentials for hyperons, low-lying charmed and bottom baryons in symmetric nuclear matter taken from Ref. [2].

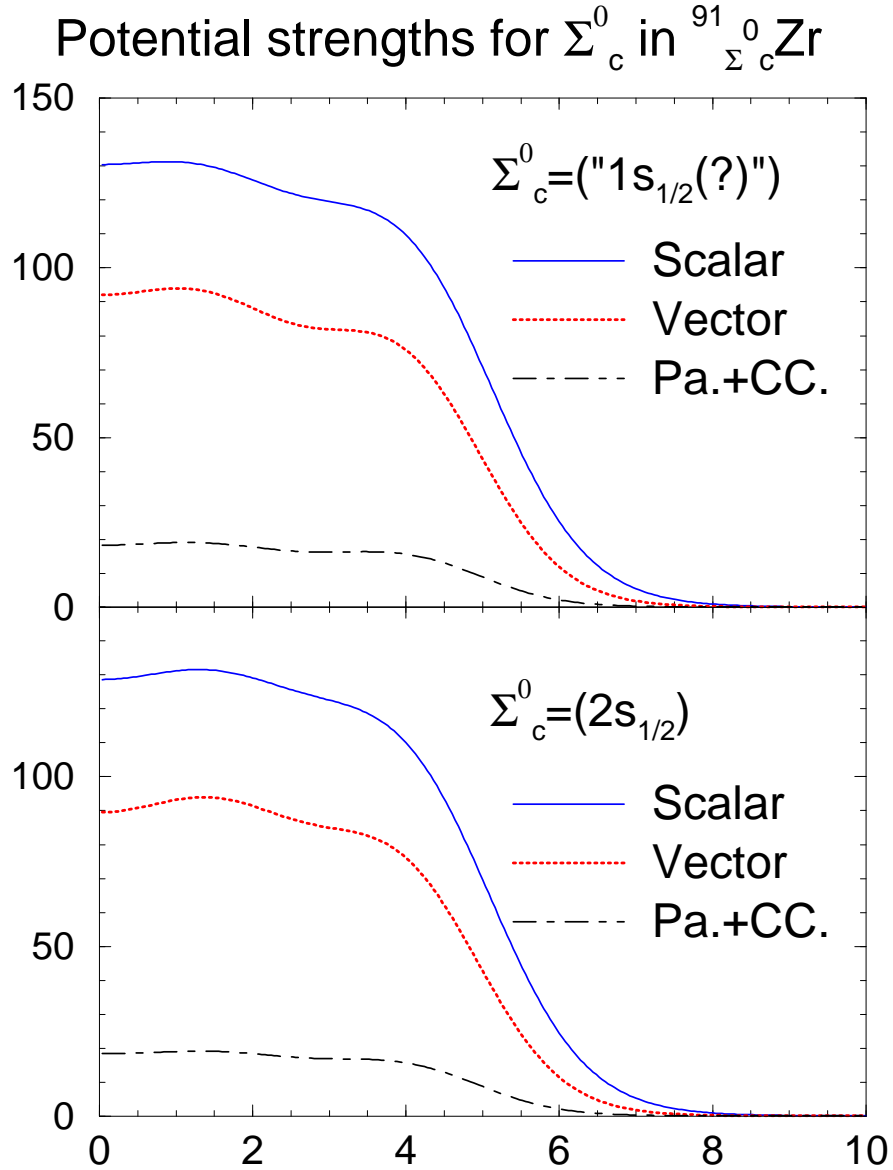


Figure 2: Potential strengths for $\Sigma_c^{0,+}$ in ${}^{91}_{\Sigma_c^0}\text{Zr}$. "Pa.+CC." stands for potential for the effective Pauli blocking plus the channel coupling effects. See the text for the meaning of " $1s_{1/2} (?)$ ".

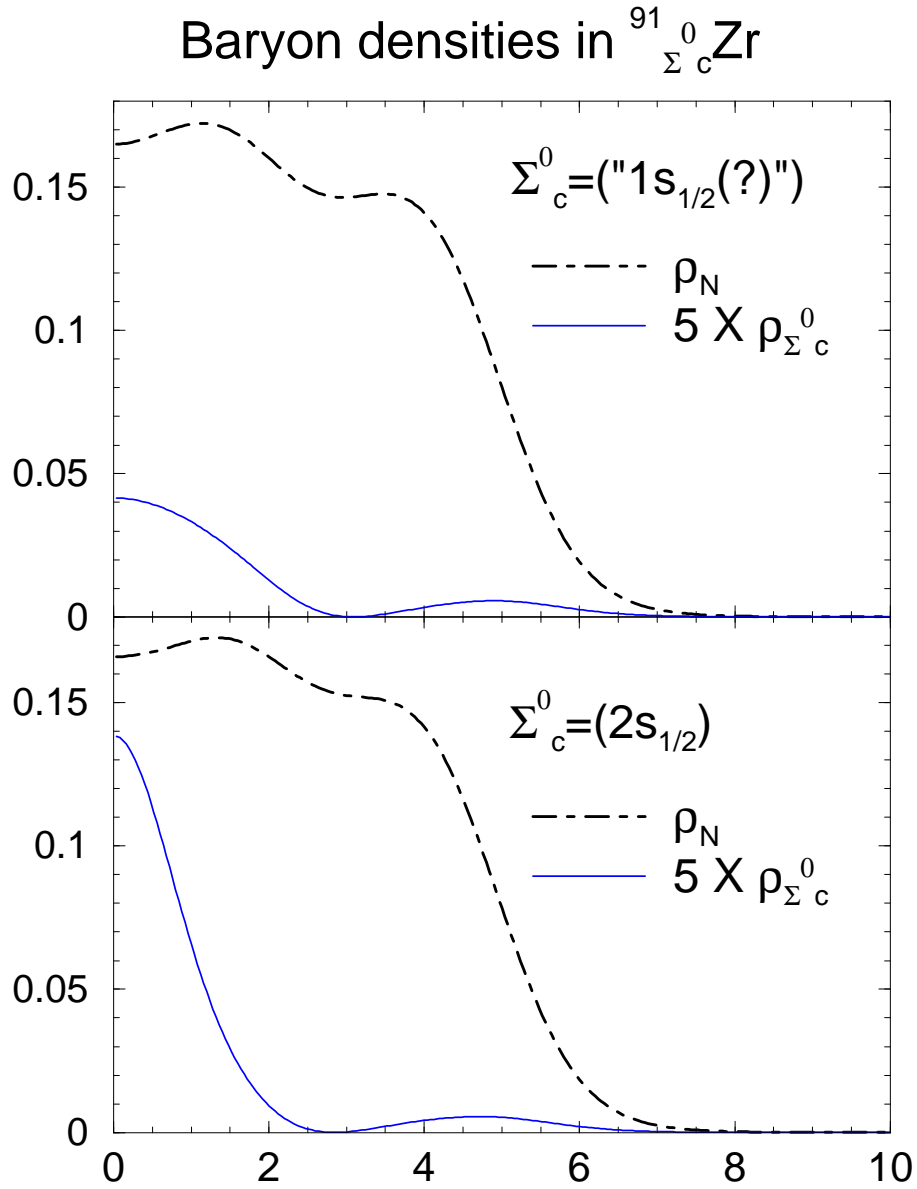


Figure 3: Baryon density distributions for the Σ_c^0 multiplied by a factor 5, and nucleons in ${}^{91}_{\Sigma_c^0}\text{Zr}$.

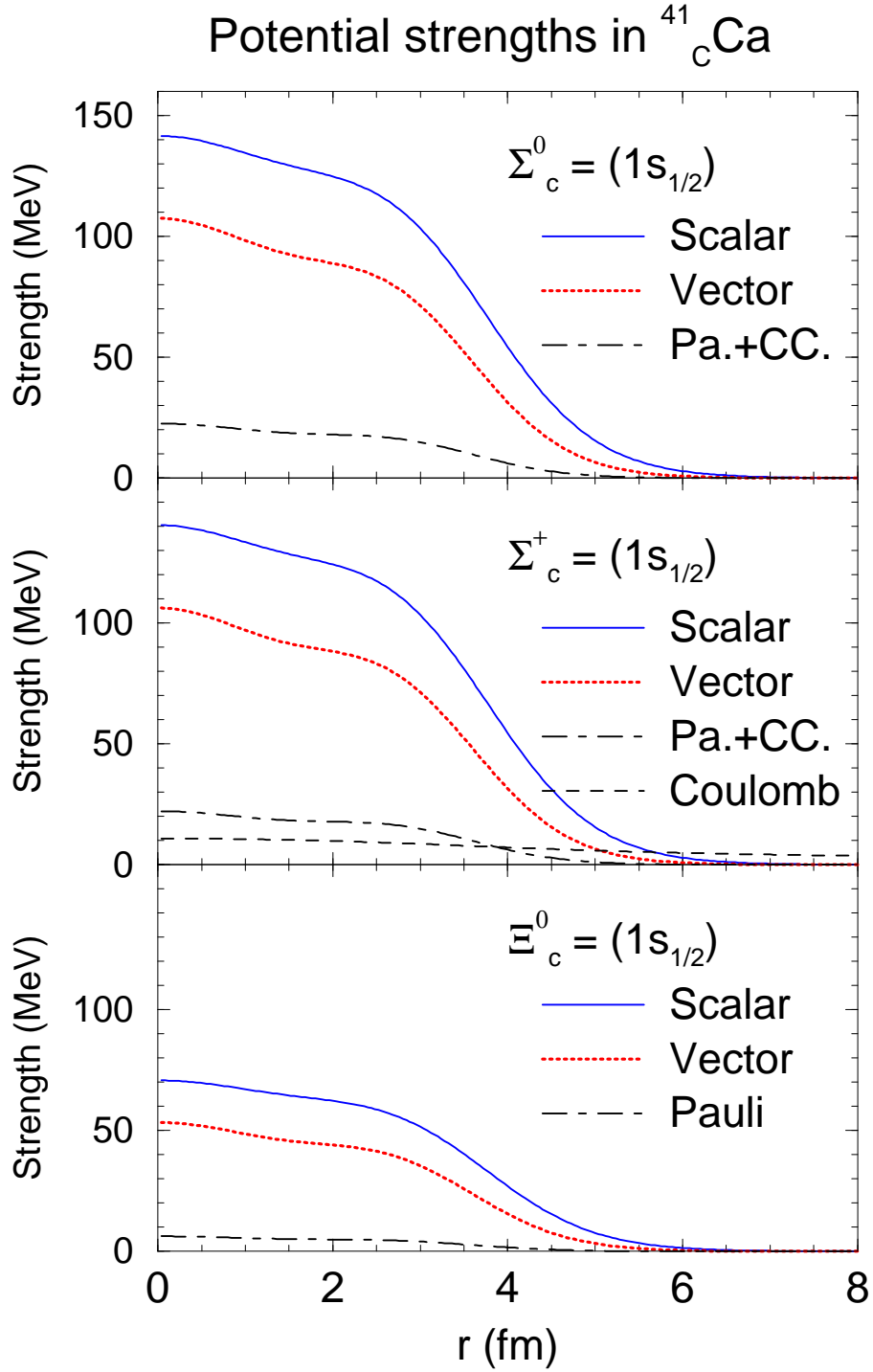


Figure 4: Potential strengths for the $\Sigma_c^{0,+}$ and Ξ_c^0 in $^{41}_j\text{Ca}$ ($j = \Sigma_c^{0,+}, \Xi_c^0$) for the $1s_{1/2}$ state. See also caption of Fig. 2.

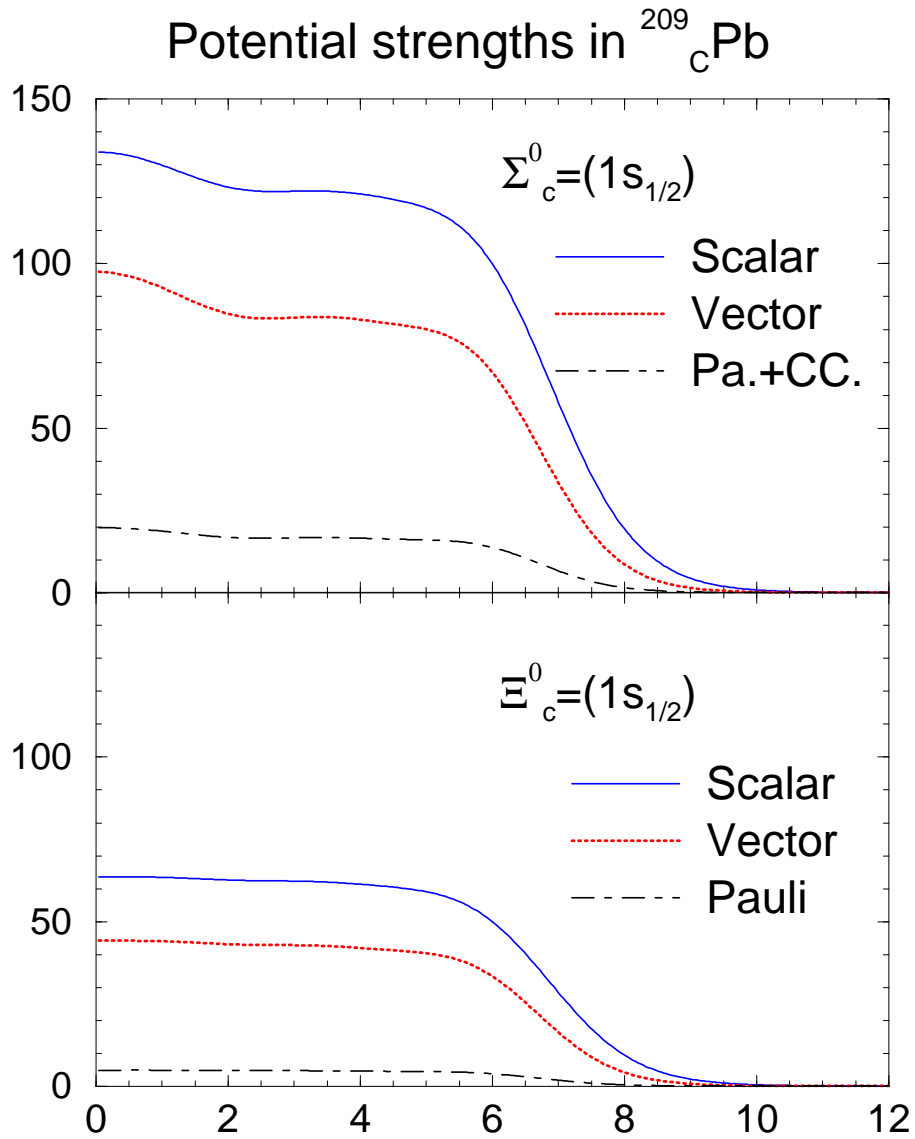


Figure 5: Potential strengths for the Σ_c^0 and Ξ_c^0 in $^{209}_j\text{Pb}$ ($j = \Sigma_c^0, \Xi_c^0$) for the $1s_{1/2}$ state. See also caption of Fig. 2.

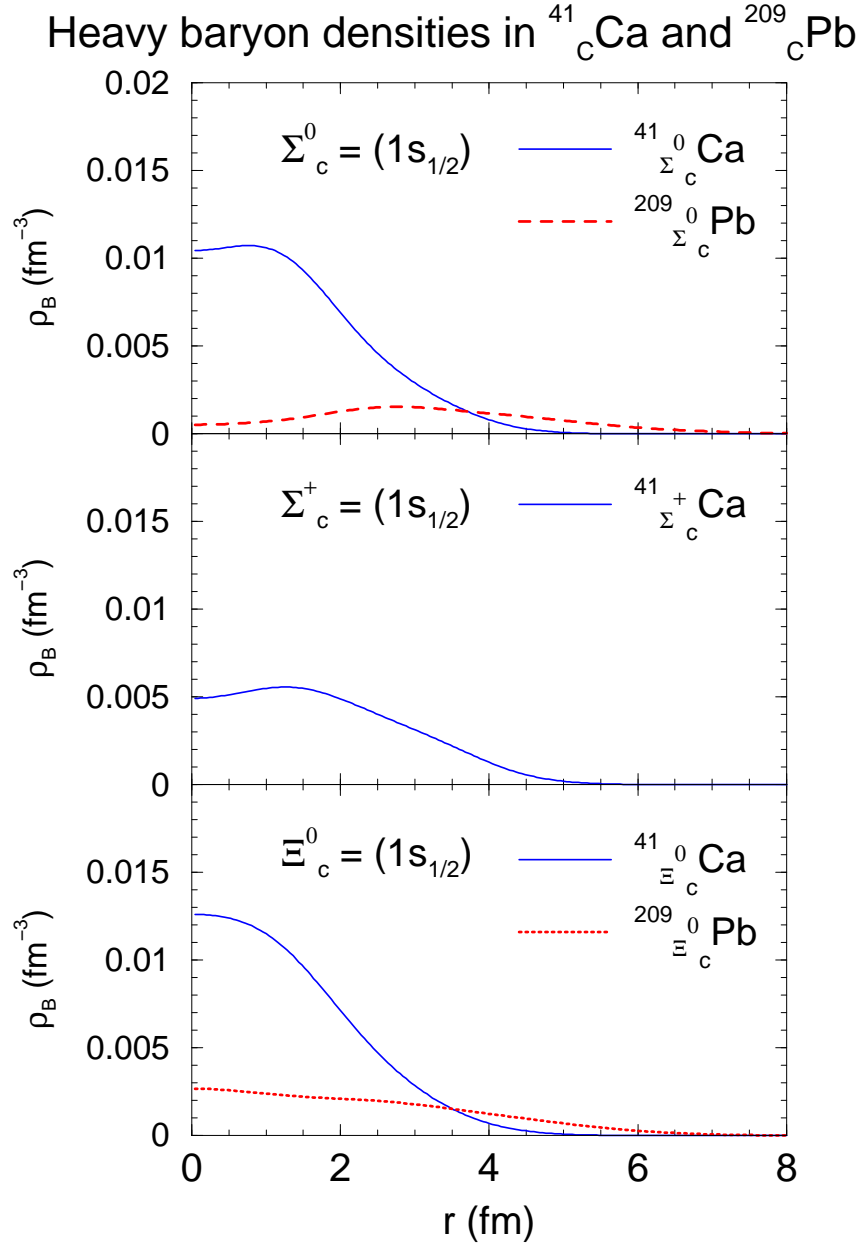


Figure 6: $\Sigma_c^{0,+}$ and Ξ_c^0 baryon (probability) density distributions for the $1s_{1/2}$ state in $^{41}_j\text{Ca}$ and $^{209}_j\text{Pb}$ ($j = \Sigma_c^{0,+}, \Xi_c^0$).